Molecular Crystals and Liquid Crystals
Publication details, including instructions for authors and subscription information:
http://www.tandfonline.com/loi/gmcl16

Electric Alignment of Liquid Crystal

W. Helfrich [a]

[a] Physics Department, F. Hoffmann-La Roche & Co., Ltd., 4002, Basle, Switzerland

Version of record first published: 21 Mar 2007.

To cite this article: W. Helfrich (1973): Electric Alignment of Liquid Crystal, Molecular Crystals and Liquid Crystals, 21:3-4, 187-209

To link to this article: http://dx.doi.org/10.1080/15421407308083319

Molecular Crystals and Liquid Crystals. 1973. Vol. 21, pp. 187–209

Electric Alignment of Liquid Crystals†

W. HELFRICH

Physics Department
F. Hoffmann-La Roche & Co., Ltd.
4002 Basle, Switzerland

Received November 11, 1972

Abstract—A survey is given of electric alignment in liquid crystals, emphasizing electro-optical effects and the physics behind them.

1. Introduction

Realignment of liquid crystals by electric fields has recently become a subject of great interest as it is the basis of a new class of electro-optical devices. The field may exert an orienting influence through the dielectric anisotropy of the liquid crystal. Another important cause of realignment is a peculiar electrohydrodynamic interaction which is also due to anisotropies. In addition, there seems to be a curvature-electric mechanism which is static, but not dielectric, and akin to piezoelectricity. Any realignment changes the optical properties of the sample because of the refractive anisotropy of liquid crystals. The following is a brief and selective review of electric alignment, describing the known electro-optical effects and outlining their physics as far as it seems understood to date. The reader is referred to other treatises(1) for an introduction to the field of liquid crystals. The list of cited original articles is not complete, its purpose is to document what is covered in the text.

The usual setup to study electrical realignment is the so-called sandwich cell consisting of two parallel plates, mostly of glass, and the liquid crystal in between. The passage of light through the sample is possible if either both plates are transparent (transmissive mode) or one transparent and the other a mirror (reflective mode). The thickness of the liquid crystal ranges typically from 10–100 μm.

---

† Plenary Lecture presented at the Fourth International Liquid Crystal Conference, Kent State University, August 21–25, 1972.

Thinner films are difficult to prepare reproducibly and thicker ones often appear turbid because of the strong light scattering of the mesophases. In most cases the electric field is directed normal to the layer. The plates serve as electrodes, being furnished with a transparent coat in the case of glass and held apart by insulating plastic spacers. A sandwich cell of this type is sketched in Fig. 1. In rare cases, parallel fields are applied, for instance by using uncoated glass in combination with metal foils as spacers and electrodes. (Field bulging is prevented, at least with dc, if the liquid crystal conducts some electricity.)

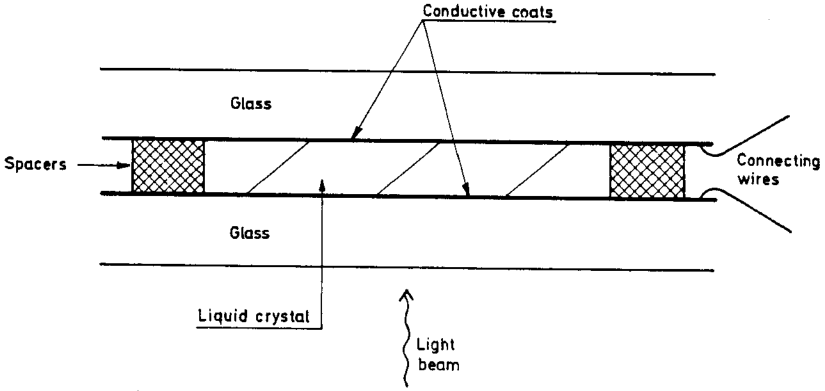

Figure 1. Diagram of a typical sandwich cell.

2. Effects in Nematics

All liquid crystals are made up of elongated molecules and represent a long-range order whose principal feature is a parallel arrangement of the long molecular axes. The nematic mesophase, to be treated first, differs from the isotropic liquid state only by this parallel ordering. It has been investigated more extensively and exhibits a larger number of electro-optical effects than the other liquid crystals.

A. DIELECTRIC ALIGNMENT

Let us start with dielectric alignment which obeys the same laws as its magnetic analogue. The three main experiments are indicated in Fig. 2. The deformations a and b have lately come to be called Freedericksz transitions.

Without field we have uniformly oriented nematic liquid crystals in cases a and b and a twisted configuration involving elastic energy in case c. The three orientation patterns are governed by the alignment on the walls. Normal orientation can be achieved by thorough cleaning or etching of the glass (coated or not) or by means of surfactants, rubbing leads to tangential alignment in its direction. An

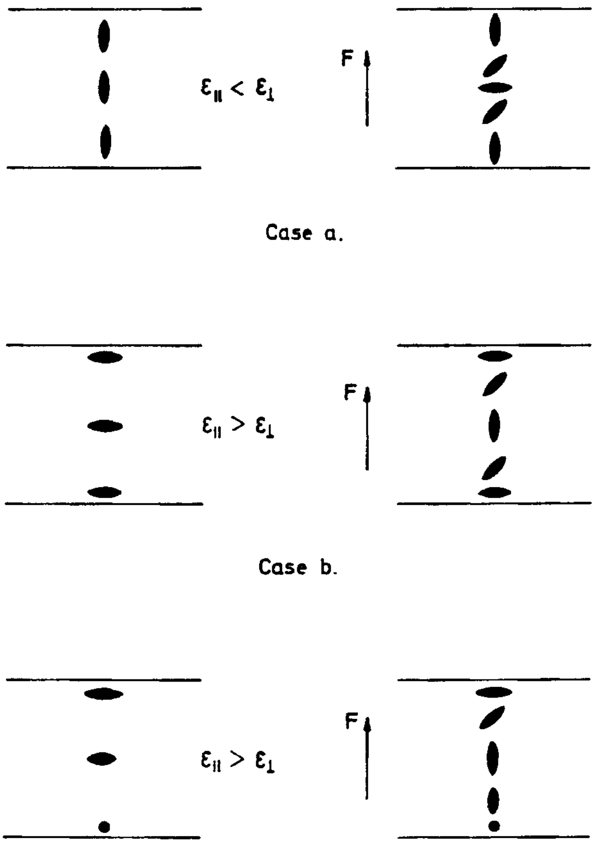

Case a.

Case b.

Case c.

Figure 2. Schematic representation of the three main experiments of dielectric realignment. The local orientation is indicated by elliptical molecules.

attempt to explain the effects of rubbing and etching in terms of local elastic energies has recently been made by Berreman.(2) Furthermore, Janning(3) has shown that depositing a coat by oblique evaporation can produce wall alignment of controlled direction.

The field causes a deflection of the nematic axis if this increases the polarization of the liquid crystal. There are two principal dielectric constants, $\epsilon_{\parallel}$ for fields parallel and $\epsilon_{\perp}$ for fields perpendicular to the nematic axis. Realignment requires either positive ($\epsilon_{\parallel} > \epsilon_{\perp}$) or negative ($\epsilon_{\parallel} < \epsilon_{\perp}$) dielectric anisotropy. Strongly polarizable liquid crystals consist of dipolar molecules, and the sign of their dielectric anisotropy is known to depend mainly on the orientation of the permanent molecular dipoles with respect to the long molecular axis. As the alignment on the walls is more or less rigid any reorientation in the bulk is opposed by liquid-crystalline elasticity which tends to preserve the original configuration and restores it when the field is turned off.

For electro-optical measurements and applications the cells of Fig. 2 have to be combined with polarizers. In discussing the three experiments we restrict ourselves to normally transmitted light. All deformations have threshold voltages of typically a few volts. Above threshold they increase gradually with the voltage (see below).

Case a (normal alignment, $\epsilon_{\parallel} < \epsilon_{\perp}$)

The deformation destroys the so-called homeotropic texture and generates a *tunable birefringence.*(4) If the cell is placed between crossed polarizers one can go from dark to light. There are also color effects just above threshold. The nematic axis must tilt in a specified direction for a uniform appearance of the cell.

Case b (parallel alignment, $\epsilon_{\parallel} > \epsilon_{\perp}$)

The deformation affects light polarized parallel to the original alignment by changing the optical thickness of the sample. It may also change the color of the light if the liquid crystal is dichroic, thus permitting *color switching.* Strong dichroism can be obtained by dissolving a dye whose molecules align with those of the host (guest–host interaction).(5) No polarizer is needed for the outgoing light.

Case c (twisted alignment, $\epsilon_{\parallel} > \epsilon_{\perp}$)

In the twisted nematic liquid crystal the plane of polarization rotates together with the nematic axis because the sample thicknesses are much larger than the wavelength of light. The incoming light should be polarized either parallel or perpendicular to the alignment on the wall in order to have a purely linear polarization all over the sample. When the electric field destroys the twisted configuration, replacing it by transition regions of splay and bend near the boundaries, the rotatory power of the cell diminishes and eventually disappears. If the cell is placed between parallel or crossed polarizers *the rotatory effect* permits one to go from dark to light or from light to dark, respectively.(6)

The standard method to derive formulas for the deformation as a function of voltage is the calculus of variation. In its general form allowing for strong realignment it involves elliptic integrals.(7) It can be shown that near the threshold the deformations are simple sinusoidal perturbations of the orientation pattern having the longest wavelength compatible with the boundary conditions. The elastic energy required and the dielectric energy released by the deformation vary, to a first approximation, as the square of the amplitude. The instability threshold is reached when the two quadratic terms are equal.

In case a the perturbation may be expressed by

$$\phi = \phi_0 \cos(\pi z/L)$$

where ϕ is the local deflection angle, ϕ_0 its amplitude, z the coordinate parallel to the field, and L the thickness of the sample extending from $z = -L/2$ to $z = +L/2$. The elastic energy per cm^2 is, for infinitesimal ϕ_0,

$$\tfrac{1}{2}K_{33}\int_{-L/2}^{+L/2}\left(\frac{\partial\phi}{\partial z}\right)^2 \mathrm{d}z = \tfrac{1}{4}K_{33}\phi_0{}^2\frac{\pi^2}{L}$$

where K_{33} is the curvature-elastic modulus for bend of the orientation lines which are everywhere parallel to the local nematic axis. The corresponding dielectric energy, i.e. the free energy released by reorientation, is

$$\tfrac{1}{2}(\epsilon_{\perp} - \epsilon_{\parallel})\epsilon_0 F^2 \int_{-L/2}^{+L/2} \phi^2\,\mathrm{d}z = \tfrac{1}{4}(\epsilon_{\perp} - \epsilon_{\parallel})\epsilon_0\phi_0{}^2F^2L$$

with F being the field strength. Equating the two energies yields the threshold field F_{th}

$$F_{\text{th}}^2 = \frac{\pi^2}{L^2}\frac{K_{33}}{(\epsilon_\perp - \epsilon_\parallel)\epsilon_0}$$

Obviously, the threshold voltage $V_{\text{th}} = F_{\text{th}} L$ is independent of sample thickness. The threshold voltages of all three main deformations may be obtained along these lines:(8)

$$\text{case a}\quad V_{\text{th}}^2 = \pi^2 \frac{K_{33}}{(\epsilon_\perp - \epsilon_\parallel)\epsilon_0}$$

$$\text{case b}\quad V_{\text{th}}^2 = \pi^2 \frac{K_{11}}{(\epsilon_\parallel - \epsilon_\perp)\epsilon_0}$$

$$\text{case c}\quad V_{\text{th}}^2 = \pi^2 \frac{K_{11} + (K_{33} - 2K_{22})/4}{(\epsilon_\parallel - \epsilon_\perp)\epsilon_0}$$

The elastic moduli K_{11} and K_{22} are for splay and twist of the orientation lines. Typically, all three Ks are of the order of 10^{-11} newton ($= 10^{-6}$ dyne).

The deformation amplitude just above threshold is derived by including in the energies terms of fourth order in ϕ_0. The procedure resembles the Landau theory of second-order phase transitions(9) and yields $\phi_0^2 \alpha (V - V_{\text{th}})$. For the amplitude ϕ_1 of the deformational wave of next higher order, $\cos(3\pi x/L)$, one obtains $\phi_1^2 \alpha (V - V_{\text{th}})^3$ which can be neglected near V_{th}. More formulas are presented in a paper by Gruler, Scheffer, and Meier(7) who use series expansions of elliptic integrals. The authors also give the change in optical thickness of the sample in cases a and b, considering weak and strong deformations. The rotation of light in case c as a function of voltage has not yet been calculated. The threshold of the optical change was found to be higher than that of the deformation,(10) as is to be expected. However, in all three main experiments the optical effect seems to be fully developed at about twice the threshold voltage of the deformation.

The relaxation time of the deformation after turning off the voltage is, for $L = 25\mu\text{m}$, typically around 0.1 sec. It varies as $\eta L^2/K$ where η is a viscosity and K a curvature-elastic modulus. The rise time decreases with increasing voltage. Relaxation is well understood,(9) but there are no formulas for the rise of the deformation from the undeformed state.

There are some observations that perpendicular wall alignment is not always rigid.(11,12) A theory for the accompanying decrease of the deformation threshold was published some time ago by Rapini and Papoular.(13) They also considered the case of rigid alignment at an angle, showing that there is no sharp threshold.

B. Electrohydrodynamic Alignment

It occurs frequently that nematic liquid crystals do not align in a direction of maximum polarizability. In particular, if the initial alignment is perpendicular to the field and the dielectric anisotropy negative ($\epsilon_{\parallel} < \epsilon_{\perp}$), the nematic axis often turns from this dielectrically stable orientation into directions almost parallel to the field. This anomalous alignment has been studied in great detail by Carr(14) and coworkers who did all their early experiments on voluminous samples, using dielectric loss measurements at very high frequencies to determine the average alignment.

Today we know that the seeming paradox results from electrohydrodynamic interaction (and in rare cases from curvature electricity; see below). The necessary space charge may, in principle, be injected from the electrodes. However, space charge can also be formed by ion segregation in the liquid crystal itself, provided the material is conducting. The conductivity need not be large, 10^{-9} Ω^{-1} cm^{-1} being usually sufficient. In general, it seems more difficult to lower excessive impurity conduction than to find suitable ionic dopants.

Charge segregation in an electric field can arise from the conductivity anisotropy which in the case of nematics is mostly positive ($\sigma_{\parallel}/\sigma_{\perp} \approx 4/3$). In addition, it is a function of the dielectric anisotropy. How charges form is indicated in the wavy orientation pattern of Fig. 3. The interaction of the applied field with the space charges will lead to material flow in alternating directions. The associated shear exerts a realigning torque on the molecules. In the steady state of electrohydrodynamic alignment this torque balances the elastic and dielectric torques.

While space charge injection is indispensable in the electrohydrodynamics of isotropic liquids, its importance in nematic phases relative to charge segregation seems not yet clear. Injection can be suppressed by the use of ac fields. A frequency of some 10 Hz is

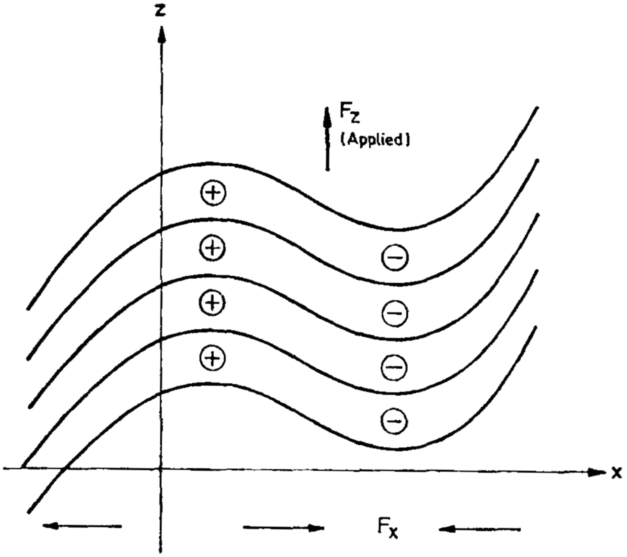

Figure 3. Charge segregation and the resulting transverse field F_x in an applied field F_z if the conductivity along the nematic axis is larger than perpendicular to it. The curves are orientation lines which are everywhere parallel to the local alignment. (From Ref. 15.)

Figure 4. Williams domains in a 38-μm thick sample of p-azoxyanisole at 130 °C and 7.8 V of *ca.* 100 Hz, as observed in unpolarized transmitted light. The microscope is focused near the top electrode. Another set of bright lines, shifted by 15.5 μm, is seen if focus is at sample bottom. (From Ref. 17.)

usually large enough to prevent both the transit of ions and the collapse of the deformation during one half period. Since the lifetime of electro-optical devices is longer with ac than with dc, ac is at present used in most applications. Injection is disregarded in the following.

In a sandwich cell with parallel wall alignment and the field across the nematic film, electrohydrodynamic alignment reveals itself by the appearance of *Williams domains*,(16) as shown in Fig. 4. The underlying orientation and flow patterns are sketched in Fig. 5. Like dielectric realignment, domain formation has a thickness-independent

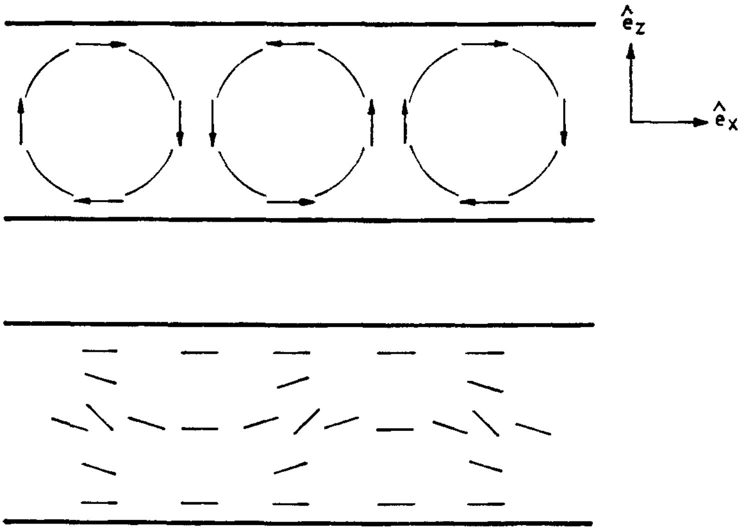

Figure 5. Cross section through the flow and orientation patterns of Williams domains, indicated by velocity vectors and rod-like molecules. (From Ref. 17.)

threshold voltage of usually a few volts. At about twice that value the domains tend to become unstable, giving way to turbulence and its optical companion, the well-known *dynamic scattering*.(18)

The first formula for the threshold voltage of domain formation(15) was derived in a one-dimensional model, the deflection angle θ varying only in x direction (see Fig. 3). Furthermore, the sample was regarded as infinite. The standard approach in stability problems is to consider infinitesimal perturbations. This decouples sinusoidal deformations and permits linearization of the forces. Accordingly, only terms linear in θ were retained in the torque densities. A threshold condition was introduced by the postulate that the distance between upward and downward flow be equal to the sample thickness L, corresponding to circular vortices in the bounded sample. The threshold voltage V_{th} is then characterized by neutral equilibrium of the torques for the orientational wave $\cos(\pi x/L)$. One obtains

$$V_{\mathrm{th}}^2 = \pi^2 \frac{K_{33}}{\dfrac{\kappa_1 \epsilon_\parallel \epsilon_0}{\eta_1}\left(\dfrac{\epsilon_\perp}{\epsilon_\parallel} - \dfrac{\sigma_\perp}{\sigma_\parallel}\right) + (\epsilon_\parallel - \epsilon_\perp)\epsilon_0 \dfrac{\sigma_\perp}{\sigma_\parallel}}$$

where κ_1 and η_1 are viscosity coefficients. This seems to agree fairly well with experiments despite the grossly simplified derivation and may serve to show in a simple way that V_{th} depends not on the magnitude but on the anisotropy of electrical conduction. There is, of course, a lower limit to σ below which counter-diffusion prevents space charge formation.

A recent computation by Penz and Ford(19) allows for the dependence of the deflection angle on two coordinates x and z (see Fig. 5) and employs an almost complete set of material constants.(20) The authors consider complex orientation waves $\theta = \theta_0 \exp(iq_x x + iq_z z)$ and calculate those q_z/q_x for which an infinitesimal perturbation is in neutral equilibrium. There can be several solutions at a given field strength. Linear combinations of these are then sought which satisfy the physical boundary conditions at given $q_x L$ and voltage. A typical result, as obtained by computer calculation, is shown in Fig. 6. The point on the left side, where the tangent is vertical, gives not only the threshold voltage of domain formation but also the ratio of domain spacing to sample thickness at threshold.

Little can be predicted on the basis of Fig. 6 about the deformation above threshold. The spacing of the domains may be invariable if there are no irregularities on the bounding walls to permit a restructuring of the orientation pattern at higher voltage. If, on the other hand, q_x is free to follow some hypothetical curve of maximum stability between the two lines indicating the instability threshold, the spacing may be a well-defined function of voltage. Such a behavior, called the *variable grating mode*,(21) was recently found by Greubel and Wolff(22) who observed that the spacing decreased with increasing voltage. The area of instability enclosed by the outer curve in Fig. 6 contains two more curves of neutral equilibrium corresponding to double and triple layers of vortices. Penz and Ford suggest that the intervention of a second instability explains the onset of turbulence.

Any calculation of the periodic deformation above threshold has to take into account that the torques are no longer linear functions of the deflection angle θ. Carroll(23) extended the one-dimensional theory by including cubic terms which represent the next higher order. He derived (not quite correctly) a formula for the voltage dependence of the amplitude of the sinusoidal deformation with fixed wave vector $q_x = \pi/L$. The procedure is analogous to that used in the case of dielectric deformations, but torques are employed instead of energies.

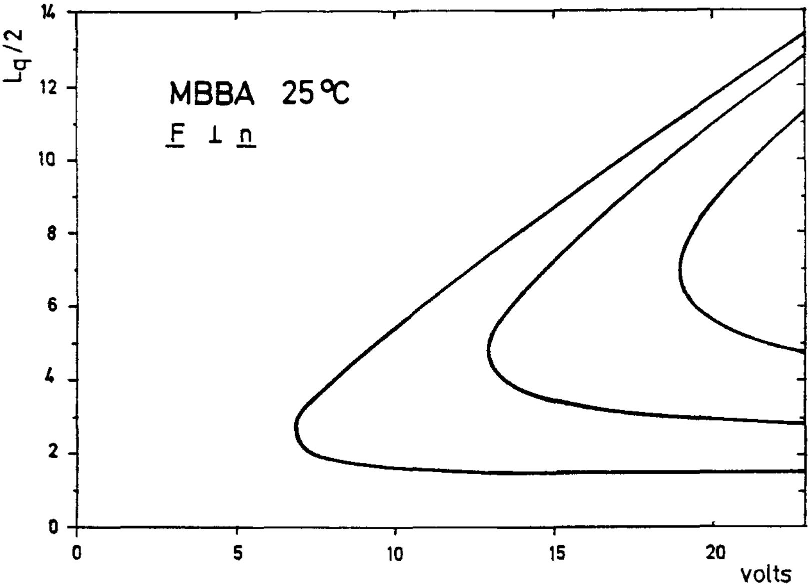

Figure 6. Curves of neutral electrohydrodynamic equilibrium as calculated for the nematic liquid crystal MBBA (p'-methoxybenzylidene-p, n-butylaniline) and for the geometry of Fig. 5. (From Ref. 19.)

In a series of experiments with parallel wall alignment the Philips group(24) examined whether the negative sign of the dielectric anisotropy is a precondition for domain formation. With one curious exception,(25) they indeed found Williams domains for $\epsilon_\parallel < \epsilon_\perp$ and dielectric realignment for $\epsilon_\parallel > \epsilon_\perp$.

It should be mentioned at this point that the wall alignment in current dynamic-scattering devices is often normal, probably because of technical difficulties with parallel alignment. Domains and turbulence also appear in this geometry with $\epsilon_{\parallel} < \epsilon_{\perp}$, but there seem to be experiments or theories.

Negative nematic conduction anisotropy was discovered by McLemore and Carr(26) and by Rondelez(27) in a material with a smectic phase at lower temperatures. Carr and coworkers(28) have done experiments, not all of them optical, to check how electrical alignment depends on the signs of both anisotropies, dielectric and conductive. Their numerous results cannot yet be easily interpreted.

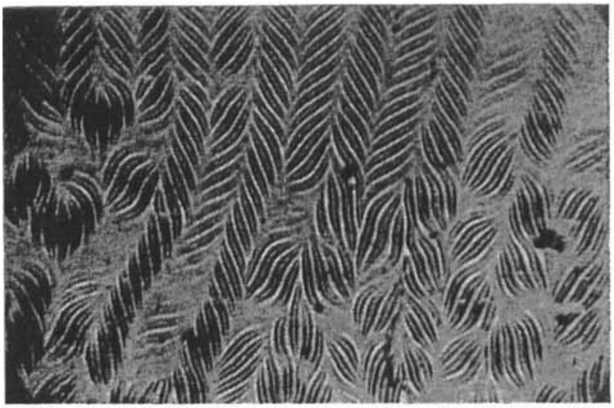

Figure 7. Chevron texture of oscillating domains in MBBA at room temperature and 260 V of 120 Hz. The distance between bright lines is 5 μm, the sample thickness 100 μm. (From Ref. 33.)

Some remarkable observations were reported by Kapustin, Trofimov and Chuvyrev. They saw slowly oscillating deformations, e.g. domains changing their direction, with both dc(29) and ac(30) excitation. It would be interesting to know if this relates to an earlier speculation(15) regarding oscillatory equilibrium at the instability threshold.

Stationary electrohydrodynamic realignment has an upper frequency limit which is roughly given by the reciprocal of a space-charge relaxation time $\tau = \epsilon\epsilon_0/\sigma$. However, at higher frequencies there may be an oscillating deformation with constant space charge.(31,32) The *oscillating domains* tend to arrange in a chevron pattern as shown in Fig. 7. A measurement of the threshold voltage versus the driving frequency in both regimes is plotted in Fig. 8.

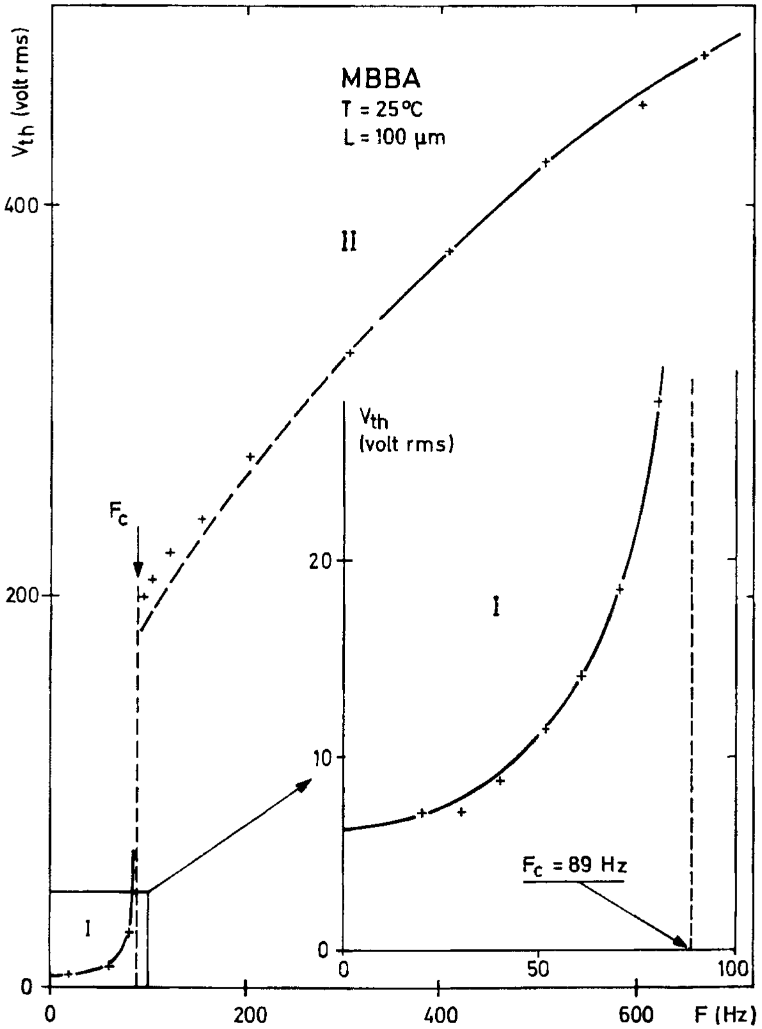

Figure 8. Typical plot of threshold voltage of domain formation vs frequency of electric field. F_c is a function of conductivity, it separates stationary and oscillating domains. (From Ref. 32.)

Like their stationary counterparts, oscillating domains are superseded by turbulence at about twice their threshold. However, the threshold is given by a critical field strength rather than a voltage and the spacing of the domains at threshold decreases with increasing frequency. There is a one-dimensional theory of oscillating domains, in particular a formula for their threshold field, which is exact if their spacing is much smaller than the sample thickness.(34) (There are no chevrons at the threshold.(33))

The relaxation time of oscillating domains can be a few msec, while 0.1 sec is typical of stationary domains at $L = 25\ \mu\text{m}$. The complete decay of the highly disordered dynamic-scattering state is slower than that of stationary domains if the turbulence generates disclinations (= line singularities).(35)

Recently, Dubois-Violette(36) has made an analysis of the transition from stationary to oscillating domains, using one-dimensional theory. The calculations indicate that with square wave excitation and, to a

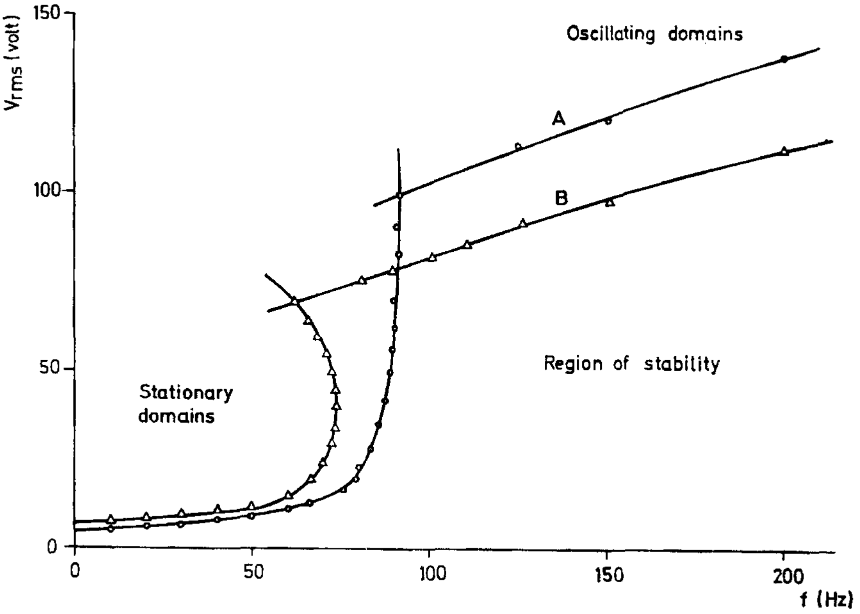

Figure 9. Experimental study of bistability at the transition from stationary to oscillating domains. A 50-μm thick sample of MBBA was excited with sine (A) and square (B) waves. (From Ref. 37.)

lesser extent, with sine waves there should be a frequency range of bistability at the transition. The prediction has been confirmed for square waves by the Orsay Liquid Crystal Group,(37) as shown in Fig. 9. That the theory yields a larger range than experiment may be due to its one-dimensionality. In a pictorial model, the second range of stability seems to be connected with the relative growth of an oscillatory component of the stationary deformation as the voltage increases above the first instability threshold. The oscillation frequency is twice that of the field, in contrast to the true oscillating domain mode where the two frequencies are equal.

C. CURVATURE-ELECTRIC ALIGNMENT

Nematic liquid crystals are nonpolar, even if they consist of polar molecules. They can, of course, be polarized by an electric field. A polarization may also arise from splay and bend deformations of the originally uniform orientation pattern. The possibility of such a curvature electricity (or piezoelectricity) was first proposed by Meyer(38) whose microscopic model based on dipolar and asymmetric molecules is reproduced in Fig. 10.

The macroscopic description of curvature electricity uses the coefficients e_{11} and e_{33} relating to splay and bend deformations, respectively. The formula for the induced polarization **P** is

$$\mathbf{P} = e_{11}\,\mathbf{n}\cdot\operatorname{div}\mathbf{n} + e_{33}(\mathbf{n}\cdot\operatorname{grad})\mathbf{n}$$

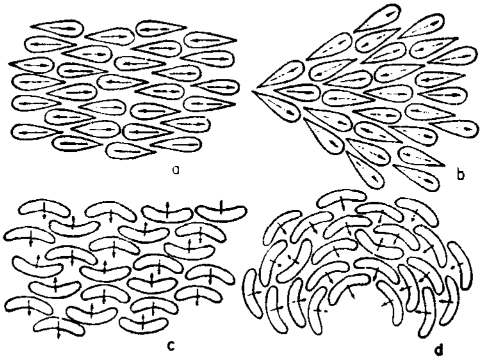

Figure 10. R. B. Meyer's model of curvature electricity. The two liquid crystals consisting of dipolar molecules are nonpolar if not deformed (a and c) but polar under splay (b) or bend (d). (From Ref. 38.)

The director **n** is a unit vector denoting the nematic axis; its polarity is physically meaningless. Another way of writing the second term is $-e_{33}\mathbf{n} \wedge \operatorname{curl}\mathbf{n}$ which shows more clearly that it refers to bending of the orientation lines. It is easy to see, microscopically and thermodynamically, that there must be a reverse effect of curvature electricity. In other words, the polarization in an electric field F produces couple stresses which cause a deformation if permitted by the boundary conditions. This may be expressed by including curvature-electric terms in Frank's formula for the curvature-elastic energy density g:

$$g = \tfrac{1}{2}K_{11}\left(\operatorname{div}\mathbf{n} - \frac{e_{11}}{K_{11}}\,\mathbf{n}\cdot\mathbf{F}\right)^2 + \tfrac{1}{2}K_{22}(\mathbf{n}\cdot\operatorname{curl}\mathbf{n})^2$$
$$+\tfrac{1}{2}K_{33}\left[(\mathbf{n}\cdot\operatorname{grad})\mathbf{n} - \frac{e_{33}}{K_{33}}\,(\mathbf{F}-\mathbf{n}(\mathbf{F}\cdot\mathbf{n}))\right]^2$$

Experimental evidence for curvature electricity has recently been reported by Schmidt, Schadt and Helfrich.⁽¹²⁾ Using a normally aligned liquid crystal (MBBA) and an electric field parallel to the nematic film, they measured the optical path difference Δl for the two principal polarizations of normally transmitted light as a function of sample thickness L and field strength F. The result,

$$\Delta l \alpha F^2 L^3,$$

is in agreement with the curvature-electric interpretation which presumes a bend deformation made possible by soft enough wall alignment. The coefficient e_{33} was deduced to be $1\cdot 10^{-12}$ A sec m^{-1} ($=4\cdot 10^{-5}$ dyne$^{1/2}$), thus being of the predicted typical order of magnitude.⁽³⁹⁾

The experimental setup was very similar to a Kerr cell. In comparison with the Kerr effect, curvature electricity permits the use of much thinner cells or lower voltages. For instance, with $L = 100\ \mu$m and $F = 100$ V cm^{-1} an optical path difference of 300 Å was observed. The drawback of curvature electricity is the slowness of liquid-crystalline reorientation, aggravated in this particular case by soft wall alignment.

Curvature electricity can also affect the dielectric and electrohydrodynamic deformations above their thresholds. As yet there are no theoretical or experimental studies of this influence which should exist, in different fashion, for dc and ac excitation.

3. Effects in Cholesterics

Cholesterics differ from nematics by the inherent tendency to form a twisted orientation pattern. They consist of chiral molecules or are obtained from nematics by dissolving such molecules. Chiral molecules are optically active, yet the extreme optical activity of cholesteric liquid crystals is a result of the twisted orientation pattern rather than molecular activity. On a small scale the molecules are parallel as in nematics, but over a larger distance the alignment axis rotates around a helical axis perpendicular to it. The pitch of the helix, i.e. the interval required for a complete rotation by 2π, varies from a few 1000 Å (in pure materials) to infinity (in mixtures).

A fascinating dielectric effect in cholesteric liquid crystals of positive small-scale dielectric anisotropy ($\epsilon_{\parallel} > \epsilon_{\perp}$) is the *unwinding of the cholesteric helix,* also called cholesteric–nematic phase transition(40) An electric field strong enough to overcome any influence of the walls, at least in the bulk of the sample, aligns the helical axis perpendicular to itself. This ensures maximum polarization without the need to destroy the twisted configuration. As the field rises the regions of alignment parallel to the field will become larger, thus increasing the pitch. Eventually, there are no wrongly aligned regions left and the orientation is uniform all over the sample.

When the field is turned off, the liquid crystal returns to the twisted state. However, the new configuration tends to be highly irregular, the orientation of the helical axis varying from place to place. It is, therefore, possible to build an electro-optical cell which strongly scatters light without field and is clear when a large enough field is applied. There is also a chromatic electro-optical effect based on the pitch-dependent Bragg reflection from the cholesteric layers.(41)

A crude formula for the critical field F_c at which unwinding is complete may be derived by equating elastic and dielectric energy densities. The exact calculation involving elliptic integrals gives(42)

$$(\epsilon_{\parallel} - \epsilon_{\perp})\epsilon_0 F_c^2 = \left(\frac{\pi}{2}\right)^2 K_{22} \left(\frac{2\pi}{P_0}\right)^2$$

and predicts correctly the dependence of pitch on field strength.(41) Here K_{22} is the twist-elastic modulus and P_0 the pitch without field. A typical value of F_c for materials of small pitch is 10^5 V cm^{-1}. F_c can be much lower for weakly twisted materials.

Another deformation of cholesteric liquid crystals is visible as a *square grid texture.*(43,44,45) It develops from the so-called planar texture in which the molecules are parallel and the helical axis perpendicular to the bounding walls of the sandwich cell. The walls are also the electrodes. A square grid texture is shown in Fig. 11. The texture has a threshold of formation and is destroyed if the field is raised to about double the threshold value. Figure 12 is a photograph of the disrupted texture. The material has a large pitch which is visible in the figure. Apparently, the helical axis has turned into directions perpendicular to the electric field.

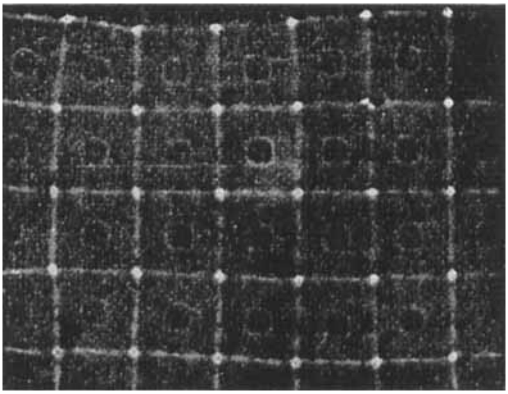

Figure 11. Square grid texture of a cholesteric liquid crystal of large pitch, as seen in transmitted light without polarizers. Distance between lines 55 μm, sample thickness 105 μm. (From Ref. 44.)

The textures of Figs. 11 and 12 resulted from electrohydrodynamic interaction. (Theory requires $\sigma_\parallel > \sigma_\perp$, see below.) They can also be obtained in a purely dielectric way if the small-scale dielectric anisotropy is positive ($\epsilon_\parallel > \epsilon_\perp$) and if space-charge formation is suppressed. The frequency limit between these two stationary modes is roughly reciprocal to the space-charge relaxation time.

An interesting electro-optical application is possible if the dielectric anisotropy is negative ($\epsilon_\parallel < \epsilon_\perp$). Starting with the clear (and optically active) planar texture, one can disrupt it electrohydrodynamically with a dc or low-frequency ac signal. The resulting turbid state can then be returned into the planar texture by applying a signal whose frequency is high enough for dielectric interaction. This memory effect which permits writing and erasing has been known for some years and was named " storage mode ".(46)

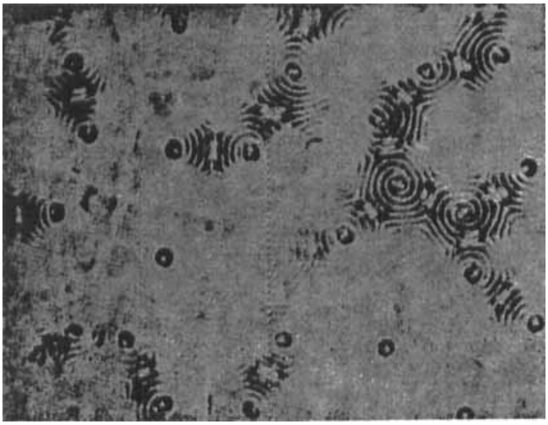

Figure 12. Disrupted texture following square grid when voltage is raised. Other conditions as in Fig. 11. (From Ref. 44.)

The formation of the square grid is well understood theoretically. At its threshold the underlying deformation consists of two orthogonal and independent one-dimensional perturbations whose orientation pattern is sketched in Fig. 13. For $P_0 \ll L$ the mean square of the theoretical threshold field is rendered very accurately by

$$F_c^2 = (6K_{22}K_{33})^{1/2}\frac{\sigma_\parallel + \sigma_\perp}{\sigma_\parallel - \sigma_\perp}\frac{\pi^2}{\epsilon_\perp \epsilon_0}\frac{1}{P_0 L}$$

with dielectric interaction, and

$$F_c^2 = (6K_{22}K_{33})^{1/2}\frac{\epsilon_\parallel + \epsilon_\perp}{\epsilon_\parallel - \epsilon_\perp}\frac{\pi^2}{\epsilon_\perp \epsilon_0}\frac{1}{P_0 L}$$

with electrohydrodynamic interaction. $\sigma_\parallel$ and $\sigma_\perp$ are the principal small-scale conductivities, K_{33} is the elastic modulus for bend. No stationary deformation can occur if the dominant anisotropy is negative. The critical field strengths are roughly the geometric mean between that of a Freedericksz transition in nematics and that of the unwinding of a cholesteric helix of pitch P_0, provided that all three experiments are carried out with the same sample thickness. The spatial period λ of the deformation is given by

$$\lambda^2 = \left(\frac{3K_{33}}{2K_{22}}\right)^{1/2} P_0 L.$$

It is independent of the type of interaction and about equal to the geometric mean of pitch and sample thickness.

The first theoretical treatment(47) of the grid pattern contained a numerical mistake. The correction, which amounts to putting a factor of 3/4 in front of K_{33} in all formulas, has been made in an extensive paper by Hurault(48) who also derives the dependence of threshold on frequency, dealing only with stationary deformations.

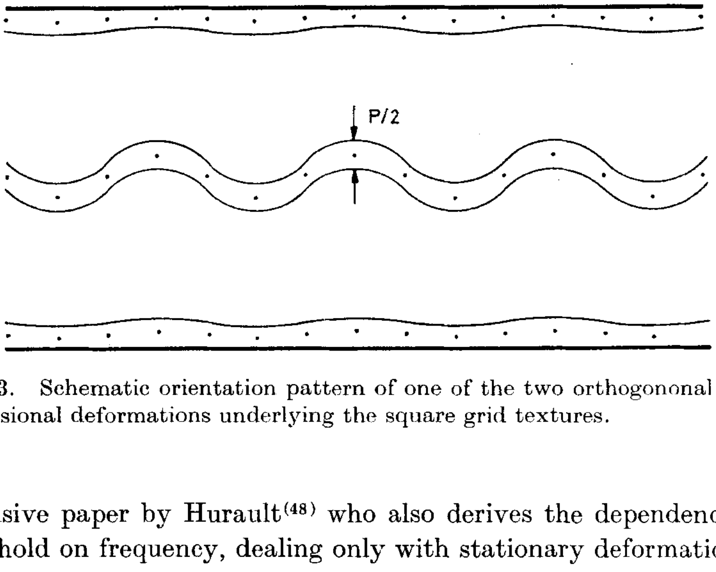

Fig. 13. Schematic orientation pattern of one of the two orthogononal one-dimensional deformations underlying the square grid textures.

In a material of negative dielectric anisotropy, Rondelez, Arnould and Gerritsma(45) saw a square grid even above the frequency of space charge relaxation. The interaction must be electrohydrodynamic and the deformation oscillating, in close analogy to oscillating domains in nematics. Frequencies which excite the oscillating deformation suppress the stationary one. The oscillating mode has a relatively high threshold field, so that lower fields can restore the planar texture as they do in the memory effect.

Deformations of cholesteric liquid crystals should relax much faster than those of nematics, in accordance with the larger voltages required for their creation. Rewinding (as opposed to unwinding) of the cholesteric helix has been studied,$^{(49)}$ and very short relaxation times (60 μsec) have, in fact, been found.

4. Effects in Smectics

Smectic liquid crystals are in some ways stiffer than nematic ones because of their more crystal-like structure. The molecules are not only ordered parallel but arranged in monomolecular layers. The long molecular axes may be aligned with the layer normal (smectic *A*, uniaxial) or at an angle (smectic *C*, biaxial). In general, smectic *A* mesophases are not easily reoriented by electric fields. The few known electro-optical effects$^{(50)}$ in sandwich cells were all found near the upper temperature limit of the smectic state and seem to be electrohydrodynamic. Carr$^{(51)}$ observed anomalous alignment in a nonoptical experiment. His smectic *A* material has a narrow temperature range and neighbors a nematic phase. All these experiments were possibly associated with disruptions of the smectic structure such as line singularities or inclusions of nematic or isotropic material.

Considering the action of magnetic fields on uniformly oriented smectic *A* films, Parodi$^{(52)}$ has recently discussed some hypothetical disrupted orientation patterns and estimated the relative probability of their formation. Rapini$^{(53)}$ has developed a theory of static deformations that are possible without disruption, dealing essentially with smectic *C*. These mesophases should be deformable in a similar way as nematics since their second axis, the one perpendicular to the layer normal, behaves like a nematic axis restricted to a certain plane. So far, no experiments to check these predictions have been reported.

5. Conclusions

Today, electric alignment of liquid crystals is an established research topic in physics. Some problems have been solved, others have been recognized and await solution. Especially a theoretical understanding of the turbulent state giving rise to dynamic scattering would be highly desirable.

Are there any new and potentially useful electro-optical effects still to be discovered which are more than modifications of those existing? We think there may be a few left, in particular in the rather varied smectic phases. A general technical aim is to build devices with orientational relaxation times much shorter than 0.1 sec. Low driving voltage and fast relaxation would be an ideal, though perhaps contradictory, combination.

REFERENCES

1. Chistyakov, I. G., *Usp. Fiz. Nauk* **89,** 551 (1966) (*Soviet Physics Uspekhi* **9,** 551 (1967)); Saupe, A., *Angew. Chemie* **80,** 99 (1968) (internat. Edit. **7,** 97 (1968)); Sackmann, H. and Demus, D., *Fortschr. Chem. Forsch.* **12,** 349 (1969); Brown, G. H., Doane, J. W. and Neff, V. D., *CRC Critical Reviews in Sol. State Sc.* **1,** 303 (1970).
2. Berreman, D. W., *Phys. Rev. Letters* **28,** 1683 (1972).
3. Janning, J. L., *Appl. Phys. Letters* **21,** 173 (1972).
4. Schiekel, M. F. and Fahrenschon, K., *Appl. Phys. Letters* **19,** 391 (1971); Kahn, F. J., *Appl. Phys. Letters* **20,** 199 (1972).
5. Heilmeier, G. H. and Zanoni, L. A., *Appl. Phys. Letters* **13,** 91 (1968).
6. Schadt, M. and Helfrich, W., *Appl. Phys. Letters* **18,** 127 (1971).
7. Gruler, H., Scheffer, T. J. and Meier, G., *Z. Naturforsch.* **27a,** 966 (1972).
8. The first derivation of the threshold in case c was given by Leslie, F. M., *Mol. Cryst. and Liq. Cryst.* **12,** 57 (1970).
9. Brochard, F., Pieranski, P. and Guyon, E., *Phys. Rev. Letters* **28,** 1681 (1972).
10. Gerritsma, C. J., De Jeu, W. H. and Van Zanten, P., *Phys. Letters* **36A,** 389 (1971).
11. Gruler, H., private communication.
12. Schmidt, D., Schadt, M. and Helfrich, W., *Z. Naturforsch.* **27a,** 277 (1972).
13. Rapini, A. and Papoular, M., *J. Phys.* **30,** C4–54 (1969).
14. See, e.g., Carr, E. F., *Mol. Cryst. and Liq. Cryst.* **7,** 253 (1969).
15. Helfrich, W., *J. Chem. Phys.* **51,** 4092 (1969).
16. Williams, R., *J. Chem. Phys.* **39,** 384 (1963). The first observation of vortical flow in connection with domains was made by Durand, G., Veyssié, M., Rondelez, F. and Leger, L., *C.R. Acad. Sci. Paris* **270B,** 97 (1970).
17. Penz, P. A., *Phys. Rev. Letters* **24,** 1405 (1970).
18. Heilmeier, G. H., Zanoni, L. A. and Barton, L. A., *Proc. IEEE* **5b,** 1162 (1968).
19. Penz, P. A. and Ford, G. W., *Phys. Rev.* **A6,** 414 (1972).
20. One of the viscosity coefficients was taken to be zero.
21. The name " variable grating mode " was proposed in Ref. 19.
22. Greubel, W. and Wolff, U., *Appl. Phys. Letters* **19,** 213 (1971).
23. Carroll, T. O., *J. Appl. Phys.* **43,** 1342 (1972).
24. De Jeu, W. H. and Gerritsma, C. J., *J. Chem. Phys.* **5b,** 4752 (1972); De Jeu, W. H., Gerritsma, C. J. and Lathouwers, T. W., *Chem. Phys.*

Letters **14**, 503 (1972); De Jeu, W. H., Gerritsma, C. J., Van Zanten, P. and Goossens, W. J. A., *Phys. Letters* **39A**, 355; Goossens, W. J. A., *Phys. Letters* **40A**, 95 (1972).

25. De Jeu, W. H., Gerritsma, C. J. and Van Boxtel, A. M., *Phys. Letters* **34A**, 203 (1971).
26. McLemore, D. P. and Carr, E. F., *J. Chem. Phys.* **57**, 3245 (1972).
27. Rondelez, F., *Sol. State Comm.*, in the press.
28. See, e.g., Flint, W. T. and Carr, E. F., to be published.
29. Kapustin, A. V., Trofimov, A. N. and Chuvyrev, A. N., *Sov. Phys.—Crystallography* **16**, 723 (1972).
30. Kapustin, A. V., Trofimov, A. N. and Chuvyrev, A. N., *Sov. Phys.—Crystallography* **17**, 157 (1972).
31. Heilmeier, G. and Helfrich, W., *Appl. Phys. Letters* **16**, 1555 (1970).
32. Orsay Liquid Crystal Group, *Phys. Rev. Letters* **25**, 1642 (1970).
33. Orsay Liquid Crystal Group, *Mol. Cryst. and Liq. Cryst.* **12**, 251 (1971).
34. Dubois-Violette, E., de Gennes, P. G. and Parodi, D., *J. Physique* **32**, 305 (1971).
35. Nehring, J. and Petty, M. S., *Phys. Letters* **40A**, 307 (1972).
36. Dubois-Violette, E., *J. Phys.* **33**, 95 (1972).
37. Orsay Liquid Crystal Group, *Phys. Letters* **39A**, 181 (1972).
38. Meyer, R. B., *Phys. Rev. Letters* **22**, 918 (1969).
39. Helfrich, W., *Z. Naturforsch.* **26a**, 833 (1971).
40. Wysocki, J. J., Adams, J. and Haas, W., *Phys. Rev. Letters* **20**, 1024 (1968).
41. Kahn, F. J., *Phys. Rev. Letters* **24**, 209 (1970).
42. de Gennes, P. G., *Sol. State Comm.* **6**, 163 (1968). A conical deformation with the helical axis parallel to the field is expected near complete unwinding if $K_{22}/K_{33} > \pi^2/4$. This condition was derived by R. B. Meyer and mentioned by de Gennes, P. G., *Mol. Cryst. and Liq. Cryst.* **7**, 325 (1969).
43. Gerritsma, C. J. and Van Zanten, P., *Phys. Letters* **37A**, 47 (1971).
44. Rondelez, F. and Arnould, H., *C.R. Acad. Sci. Paris* **273B**, 549 (1971).
45. Rondelez, F., Arnould, H. and Gerritsma, C. J., *Phys. Rev. Letters* **28**, 735 (1972). The transition between the dielectric and electrohydrodynamic stationary regimes was also studied by Scheffer, T. J., *Phys. Rev. Letters* 593 (1972).
46. Heilmeier, G. H. and Goldmacher, J. E., *Appl. Phys. Letters* **13**, 132 **28**, (1968).
47. Helfrich, W., *J. Chem. Phys.* **55**, 839 (1971).
48. Hurault, J. P., *J. Chem. Phys.*, in the press.
49. Jakeman, E. and Raynes, E. P., *Phys. Letters* **39A**, 69 (1972).
50. Vistin, L. K. and Kapustin, A. V., *Sov. Phys.—Crystallography* **13**, 284 (1968); Arora, S. L., Fergason, J. L. and Saupe, A., *Mol. Cryst. and Liq. Cryst.* **10**, 243 (1970); Castellano, J., private communication.
51. Carr, E. F., *Mol. Cryst. and Liq. Cryst.* **13**, 27 (1971).
52. Parodi, O., *Sol. State Comm.*, in the press.
53. Rapini, A., *J. Physique* **33**, 237 (1972).